

# Highly Dispersed TaO<sub>x</sub> Nanoparticles Prepared by Electrodeposition as Oxygen Reduction Electrocatalysts for Polymer Electrolyte Fuel Cells

Jeongsuk Seo,<sup>†</sup> Lan Zhao,<sup>‡</sup> Dongkyu Cha,<sup>‡</sup> Kazuhiro Takanabe,<sup>§</sup> Masao Katayama,<sup>†</sup> Jun Kubota,<sup>†,||</sup> and Kazunari Domen<sup>\*,†</sup>

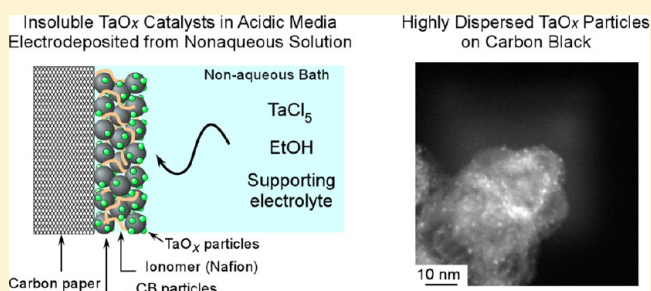
<sup>†</sup>Department of Chemical System Engineering, The University of Tokyo, 7-3-1 Hongo, Bunkyo-ku, Tokyo 113-8656, Japan

<sup>‡</sup>Advanced Nanofabrication, Imaging and Characterization Laboratory, King Abdullah University of Science and Technology (KAUST), Thuwal 23955-6900, Saudi Arabia

<sup>§</sup>Division of Chemical and Life Sciences and Engineering, KAUST Catalysis Center (KCC), King Abdullah University of Science and Technology (KAUST), 4700 KAUST, Thuwal 23955-6900, Saudi Arabia

<sup>||</sup>Elements Strategy Initiative for Catalysts and Batteries (ESICB), Kyoto University, Katsura, Kyoto 615-8520, Japan

**ABSTRACT:** Based on the chemical stability of group IV and V elements in acidic solutions, TaO<sub>x</sub> nanoparticles prepared by electrodeposition in an ethanol-based Ta plating bath at room temperature were investigated as novel nonplatinum electrocatalysts for the oxygen reduction reaction (ORR) in polymer electrolyte fuel cells (PEFCs). Electrodeposition conditions of Ta complexes and subsequent various heat treatments for the deposited TaO<sub>x</sub> were examined for the best performance of the ORR. TaO<sub>x</sub> particles on carbon black (CB), electrodeposited at a constant potential of  $-0.5\text{ V}_{\text{Ag/AgCl}}$  for 10 s and then heat-treated by pure H<sub>2</sub> flow at 523 K for 1 h, showed excellent catalytic activity with an onset potential of  $0.93\text{ V}_{\text{RHE}}$  (for  $2\text{ }\mu\text{A cm}^{-2}$ ) for the ORR. Surface characterizations of the catalysts were performed by scanning transmission electron microscopy (STEM), transmission electron microscopy (TEM), and energy dispersive X-ray spectroscopy (EDS). The loading amounts of the electrodeposited material on the CB were determined by inductively coupled plasma atomic emission spectroscopy (ICP-AES). All the physical results suggested that high dispersion of TaO<sub>x</sub> particles on the CB surface with 2–3 nm size was critical and key for high activity. The chemical identity and modified surface structure for the deposited TaO<sub>x</sub> catalysts before and after H<sub>2</sub> heat treatment were analyzed by X-ray photoelectron spectroscopy (XPS). The formation of more exposed active sites on the electrode surface and enhanced electroconductivity of the tantalum oxide promoted from the H<sub>2</sub> treatment greatly improved the ORR performance of the electrodeposited TaO<sub>x</sub> nanoparticles on CB. Finally, the highly retained ORR activity after an accelerated durability test in an acidic solution confirmed and proved the chemical stability of the oxide nanoparticles. The high utilization of the electrodeposited TaO<sub>x</sub> nanoparticles uniformly dispersed on CB for the ORR was comparable to that of commercial Pt/CB catalysts, visually demonstrating their catalytic potential for PEFC electrocatalysts.



## 1. INTRODUCTION

In order to reduce the high cost of Pt or Pt-based catalysts, which have thus far been employed almost exclusively as fuel cell electrodes, the development of non-platinum catalysts is essential for extensive and commercial applications particularly of polymer electrolyte fuel cells (PEFCs) in vehicles and residential cogeneration systems. N-coordinated Fe- and Co-based complexes as candidates for nonplatinum catalysts have been reported to be effective electrocatalysts for the oxygen reduction reaction (ORR).<sup>1–3</sup> However, Rabis et al. have shown the periodic table indicating the most stable substances in typical PEFC cathode conditions at 80 °C,<sup>4</sup> and the iron group elements seem to be unstable because they are essentially susceptible to dissolution in acidic solutions.

Another promising portion of the periodic table for this application is represented by the group IV and V elements. Elements such as Ti, Zr, Ta, and Nb are known to be chemically stable under acidic conditions. Several compounds based on these elements have been reported as ORR electrocatalysts.<sup>5–15</sup> These compounds have been explored to improve electrocatalytic activity for ORR by doping with other compounds or by various heat treatments. Despite many attempts, oxides, nitrides, carbides, and their mixture compounds based on Ta, Nb, and Zr have thus far shown limited catalytic activity and poor long-term stability for fuel

Received: February 6, 2013

Revised: April 17, 2013

Published: April 29, 2013

cell applications. In particular, nitrides or catalysts doped with nitrogen with high electroconductivity and long-term stability for ORR have not been reported, even though several catalysts have shown acceptable results for non-platinum cathode catalysts.<sup>13</sup> The reason for this might be the fact that they basically tend to change into the oxide form, that is, the most stable substance under PEFC acidic conditions.<sup>4</sup> In fact, oxides have been commonly known to be stable materials in an acidic atmosphere. Unfortunately, the most stable oxides with maximum valency have poor electroconductivity, which means they should have low ORR activity.<sup>16</sup>

The conventional synthesis of compounds based on the group IV–V elements has considerable disadvantage for non-platinum electrocatalysts because the catalyst particles are easily aggregated and frequently form large sizes over 100 nm as a consequence of the high-temperature preparation needed.<sup>5–9</sup> Our group has therefore developed preparation methods for well-dispersed group IV–V catalysts in the nanoscale using the polymer complex method,<sup>10</sup> a dry sputtering process,<sup>11</sup> and the mesoporous graphitic (mpg) C<sub>3</sub>N<sub>4</sub> method.<sup>12,13</sup> These attempts have enabled us to prepare well-dispersed, nanoscale metal compounds supported on carbon black (CB) particles with diameter of 30–40 nm.

Electrodeposition is one of the most powerful techniques to obtain uniformly dispersed nanoparticles on conductive supports.<sup>17–20</sup> It has also been reported to be effective to form desirable three-phase boundaries required for electrochemical reactions of PEFCs because the catalysts are selectively deposited at the active areas on the support.<sup>17,19</sup> Most of these results have been limited to Pt or Pt-based catalysts electrodeposited under aqueous solutions. However, group IV–V metal complexes are not soluble in aqueous solutions because they form oxides or hydroxide precipitates by reacting with H<sub>2</sub>O.<sup>21</sup> The electrodeposition of metallic Ta has been rarely performed by applying strongly negative potentials on substrates in molten salts at ca. 1073 K<sup>22</sup> or ionic liquids at 373–473 K,<sup>23–25</sup> even under high pressure. Consequently, Ta species was electrodeposited as metallic species with a several-micrometer-thick layer.<sup>22–25</sup> Based on their chemical stability in acidic solutions, Ta oxide nanoparticles well-dispersed on substrates are preferred for PEFC cathode electrocatalysts since the deposition of only a few atomic layers can form efficient active sites. Experimentally, the electrodeposition of Ta oxide nanoparticles, not metallic Ta, is expected under mild deposition conditions such as a suitable potential, room temperature, and the use of a general solvent. With this background, our group has recently demonstrated that highly dispersed nanoscale Ta oxide catalysts could be prepared by electrodeposition in an ethanol-based Ta plating bath at room temperature, and the catalysts showed excellent catalytic activity for the ORR.<sup>26</sup>

In the present study, we have greatly extended the development of catalytic performance and have carried out detailed physical analysis for highly dispersed TaO<sub>x</sub> nanoparticles without N on CB supports prepared by potentiostatic electrodeposition. Specifically, the electrodeposition behavior of Ta complexes in a nonaqueous Ta plating solution were observed for the optimization of the deposition conditions necessary to design the best electrode structure for outstanding ORR performance. The influence of heat treatments applied to the catalysts, after electrodeposition, on improved catalytic activity for the ORR was studied by applying different heating times, temperatures, and gas atmospheres. X-ray photoelectron

spectroscopy (XPS) analysis was used to discuss the exact chemical identity of the TaO<sub>x</sub> catalysts electrodeposited onto CB surfaces. As one of the most important factors for electrocatalysts for PEFC cathodes, long-term stability of the TaO<sub>x</sub> nanoparticles was evaluated under typical acidic conditions in addition to comparison of ORR activity with commercial Pt/CB catalysts.

## 2. EXPERIMENTAL SECTION

**2.1. Preparation of TaO<sub>x</sub> Catalysts on Bare CB Electrodes by Electrodeposition.** Bare electrodes were first prepared using CB powders. The CB powders (Vulcan-XC72 or Ketjen Black EC-600JD) were mixed with a proton ionomer solution (Nafion, Aldrich 1100EW, 5 wt % in water/aliphatic alcohols) and isopropyl alcohol (IPA, 99.9%, Kanto Chemical). The composition ratio of the CB to the ionomer solution was fixed at 2:3 in terms of weight. For high dispersion, the mixed CB slurry was repeatedly placed in an ultrasonic bath and on a magnetic stirrer. Subsequently, the well-dispersed CB slurry was sprayed onto carbon paper (10 mm × 10 mm) pretreated with polytetrafluoroethylene (EC-TP1-060T, Toyo Corporation) on a hot plate at 343 K. The three-dimensional CB layer was loaded on the carbon paper with 0.5 mg cm<sup>-2</sup>. The bare CB electrodes were completely dried on the hot plate for 30 min to evaporate the remaining solvent after spraying.

Next, the potentiostatic deposition of Ta species was performed in a three-electrode system with a potentiostat (HZ5000, Hokuto Denko). The bare CB electrode as the working electrode was immersed in a nonaqueous Ta plating bath containing a Ta precursor, 20 mM TaCl<sub>5</sub> (97.0%, Kanto Chemical), and a supporting electrolyte, 20 mM NaClO<sub>4</sub> (99%, Sigma-Aldrich), with an anhydrous ethanol solvent. A carbon rod was used as a counter electrode to avoid Pt contamination. An Ag/AgCl electrode (HX-R4, Hokuto Denko) was mounted as a reference electrode. A constant potential of -1.0, -0.7, -0.5, and -0.3 V<sub>Ag/AgCl</sub> was applied to the bare carbon electrode for 10 s at room temperature for electrodeposition. After the electrodeposition, the electrodes were fully washed with ethanol to remove the residues of the Ta precursor and thoroughly dried. Finally, the Ta-electrodeposited electrodes were heat-treated by varying the temperature as 473, 523, and 573 K and the heating time from 30 min to 2 h in various atmospheres under pure H<sub>2</sub>, N<sub>2</sub>, or NH<sub>3</sub> flow at a heating rate of 5 K min<sup>-1</sup>. The concept of an electrode is illustrated in Figure 1. The CB particles adhered to the carbon substrate and other particles and Ta species were electrodeposited on the bare CB surfaces.

The ORR activity for the TaO<sub>x</sub> catalysts by electrodeposition was compared with that of the commercial Pt/CB catalysts. For preparing the Pt/CB catalyst, commercial 20 wt % Pt/CB (EC-20-PTC, Electrochem, Inc., Pt on the Vulcan XC-72R) was mixed with an ionomer solution and IPA, and the slurry was then sprayed on the bare CB electrode by fixing the loading amounts of Pt to 0.025 mg cm<sup>-2</sup>.

**2.2. Electrochemical Measurements.** First, the deposition behavior of Ta species on a glassy carbon (GC) electrode was studied under the same environment with a nonaqueous Ta plating solution and a standard three-electrode system for the electrodeposition. Cyclic voltammetry for the reduction reaction of Ta complexes on GC was performed by sweeping the potential from 1.0 to -1.0 V<sub>Ag/AgCl</sub> under an Ar-saturated

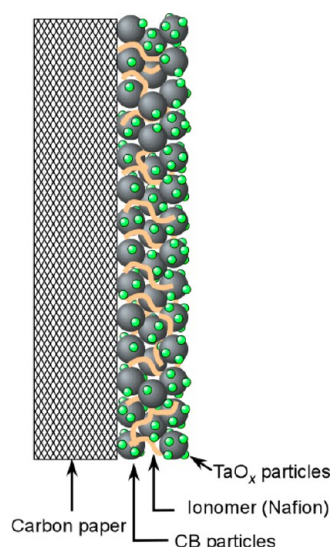


**Figure 1.** Schematic of TaO<sub>x</sub> particles loaded on a bare CB electrode after electrodeposition.

atmosphere at 298 K. The cyclic voltammogram was generally recorded at a scan rate of 5 mV s<sup>-1</sup>.

To evaluate ORR activities of the electrodeposited TaO<sub>x</sub> catalysts, electrochemical measurements were carried out in a conventional single-vessel electrochemical cell with an Ag/AgCl reference and carbon counter electrodes. Linear sweep voltammograms for the ORR were obtained in the potential range of 1.23–0.20 V<sub>RHE</sub> for the cathodic direction with a scan rate of 5 mV s<sup>-1</sup> in a 0.1 M H<sub>2</sub>SO<sub>4</sub> aqueous solution at 298 K under the purging of Ar and O<sub>2</sub> gases at 1 atm. The difference in current density between the O<sub>2</sub>-saturated and Ar-saturated atmosphere is considered to correspond exactly to the real catalytic activity for the ORR, *i*<sub>ORR</sub>. The Ag/AgCl reference electrode was calibrated in a 0.1 M H<sub>2</sub>SO<sub>4</sub> aqueous solution at 298 K to a reversible hydrogen electrode (RHE) which consisted of a Pt electrode and H<sub>2</sub> at 1 atm; the potential in a 0.1 M H<sub>2</sub>SO<sub>4</sub> solution in this paper is expressed in RHE.

For a stability test of the electrodeposited TaO<sub>x</sub> catalysts, the cathodic potential sweep was cycled at 0.6–1.23 V<sub>RHE</sub> with accelerated cathodic and anodic scan rates of 50 mV s<sup>-1</sup> for 1000 times in 0.1 M H<sub>2</sub>SO<sub>4</sub> under an O<sub>2</sub>-saturated atmosphere at 298 K. The ORR activities for the current density at 0.60 V<sub>RHE</sub> were measured in the potential range from 1.23 to 0.20 V<sub>RHE</sub> for the cathodic direction under an O<sub>2</sub>-saturated atmosphere with a scan rate of 5 mV s<sup>-1</sup> at 298 K after every 50 accelerated cycles.

**2.3. Surface and Physical Characterizations.** The surface morphology and elemental composition for the TaO<sub>x</sub>-electrodeposited electrodes were characterized by scanning transmission electron microscopy (STEM; TITAN ST, FEI), transmission electron microscopy (TEM; TITAN ST, FEI), scanning electron microscopy (SEM; S-4700, Hitachi), and energy dispersive X-ray spectroscopy (EDS; EMAX-7000, Horiba). The loading amounts of the deposited Ta on the CB electrode were determined by inductively coupled plasma atomic emission spectroscopy (ICP-AES). The chemical identity and modified surface structure for the deposited TaO<sub>x</sub> catalysts before and after H<sub>2</sub> heat treatment were analyzed by X-ray photoelectron spectroscopy (XPS; JPS-90SX, JEOL) using a nonmonochromatized X-ray source with a Mg Kα anode, emission current 10 mA, and an acceleration voltage

of 8 kV. The binding energies were calibrated using Au 4f<sub>7/2</sub> at 83.8 eV to compensate for the electrostatic charging. For the internal compositions of the TaO<sub>x</sub> nanoparticles, Ar<sup>+</sup> ion bombardment was performed to remove the surface layer adsorbed on the surface of the electrode. Finally, the crystal structure of the Ta<sub>3</sub>N<sub>5</sub> catalysts deposited on the PEG-bonded CB electrode was investigated by X-ray diffraction (XRD; RINT-UltimaIII, Rigaku).

### 3. RESULTS AND DISCUSSION

**3.1. Electrodeposition Behavior of Ta Complexes on Glassy Carbon under Ar Atmosphere.** The electrochemical behavior of the Ta species was characterized for optimizing the electrodeposition. It has generally been known that the electrodeposition patterns are influenced by the deposition conditions used, such as the substrate used, the type of ligand, the electrolyte, and the oxidation states of the deposited species. In order to screen the electrodeposition patterns of Ta species on carbon, GC electrodes with an area of 1 cm<sup>2</sup> were applied as the substrate for the electrodeposition. TaCl<sub>5</sub> and NaClO<sub>4</sub> were used as the Ta precursor and the supporting electrolyte, respectively. A nonaqueous Ta plating bath based on ethanol was selectively chosen to prevent the reaction of TaCl<sub>5</sub> powder with H<sub>2</sub>O into Ta<sub>2</sub>O<sub>5</sub> directly. Consequently, Ta(V) complexes in the Ta(OC<sub>2</sub>H<sub>5</sub>)<sub>5</sub>-based solution, produced from TaCl<sub>5</sub> dissolution in ethanol as represented by eq 1, are expected to be electrochemically deposited on carbon.

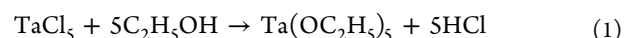
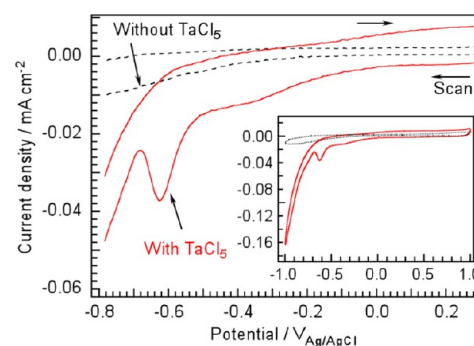


Figure 2 shows the cyclic voltammetry behavior of the GC electrode in the nonaqueous plating solutions with and without



**Figure 2.** Cyclic voltammograms of a GC electrode in a nonaqueous Ta plating bath in an Ar-saturated atmosphere. The Ta plating bath included 20 mM TaCl<sub>5</sub> and 20 mM NaClO<sub>4</sub> in ethanol solvent. The dashed (black) and solid (red) lines show the electrochemical behaviors without and with 20 mM TaCl<sub>5</sub>, respectively. The inset indicates voltammograms swept in the whole potential range between 1.0 and -1.0 V<sub>Ag/AgCl</sub> at a scan rate of 5 mV s<sup>-1</sup>.

a Ta precursor, TaCl<sub>5</sub>, under an Ar-saturated atmosphere at room temperature. During the first cathodic sweep, cyclic voltammograms were recorded in the potential range of -1.0 to 1.0 V<sub>Ag/AgCl</sub> with a scan rate of 5 mV s<sup>-1</sup>. In the solution without Ta species, no significant peaks are observed, as shown in Figure 2 (dashed line). The small cathodic current in the only supporting electrolyte was observed below -0.25 V<sub>Ag/AgCl</sub>, which was presumably due to the reduction of H<sup>+</sup> from the H<sub>2</sub>O impurity in ethanol or NaClO<sub>4</sub>. In the Ta plating solution (solid line), two reduction peaks exist: one a weakly broad peak around -0.35 V<sub>Ag/AgCl</sub> and the other a sharper peak at -0.63



$V_{\text{Ag/AgCl}}$ . In a much more negative potential sweep, the cathodic current is largely increased up to  $-1.0 V_{\text{Ag/AgCl}}$ . For an anodic scan, the anodic current was observed above  $-0.25 V_{\text{Ag/AgCl}}$ , but there were no specific peaks corresponding to the two cathodic peaks. Among tantalum chlorides,  $\text{TaCl}_5$ ,  $\text{TaCl}_4$ , and  $\text{TaCl}_3$  are known to be stable compounds.<sup>24,27</sup> It has been reported that electrodeposited Ta is reduced to metallic elemental Ta via Ta(IV) and Ta(III).<sup>24,25,28–31</sup> Thus, the weak broad peak at  $-0.35 V_{\text{Ag/AgCl}}$  is regarded as the reduction of Ta(V) to Ta(IV). In the reversed anodic scan, the oxidation current above  $-0.25 V_{\text{Ag/AgCl}}$  presumably indicates incomplete stripping of the deposited Ta species during the cathodic sweep. The more negative peak at  $-0.63 V_{\text{Ag/AgCl}}$  is related to reduction to Ta(III), and this reaction seems to be irreversible because of the absence of anodic peaks corresponding to the cathodic peak. The continuously increasing cathodic current below  $-0.7 V_{\text{Ag/AgCl}}$  might be from  $\text{H}_2$  evolution. This is because a byproduct, HCl, as a source of  $\text{H}^+$  was formed from the reaction of  $\text{TaCl}_5$  and ethanol. It would not be possible to reduce Ta(V) to a metallic state Ta(0) even if it is swept to a much more negative potential than  $-2.0 V_{\text{Ag/AgCl}}$ .<sup>24,25,28–31</sup> It is proposed that the Ta(V) ethoxide in the ethanol solution is reduced to Ta(IV) or Ta(III), resulting in deposition or adsorption on CB surfaces. Confirmation of the electrodeposition of Ta species will be further discussed in sections 3.2 and 3.5. Most possible states of the electrodeposited Ta on CB should be oxides or hydroxides after exposure of the catalysts in humid air because there is no source of nitrogen or carbon to form nitrides and carbides and because hydroxide itself may dissociate in an acidic media. Thus, the Ta-electrodeposited catalysts are expressed as  $\text{TaO}_x$  in this paper. The advantage of electrodeposition is that Ta species are selectively deposited on the electroconductive CB surfaces, but not on the insulating  $\text{TaO}_x$  particles. This suppresses the growth of insulating  $\text{TaO}_x$  particles and promotes the high dispersion of  $\text{TaO}_x$  nanoparticles on the conductive CB surfaces.

**3.2. ORR Activities of  $\text{TaO}_x$  Catalysts Electrodeposited on Carbon Black under Various Potentials.** According to the electrochemical behavior of Ta species, the applied potential, which is one of the critical electrodeposition parameters, was first examined for the deposition of Ta species onto bare CB electrodes. Various potentials were applied to the bare carbon electrodes for 10 s under the nonaqueous  $\text{Ta}(\text{OC}_2\text{H}_5)_5$ -based solution. Figure 3a representatively shows cyclic voltammograms in an Ar atmosphere for the  $\text{TaO}_x$  catalysts deposited at the potential of  $-0.5 V_{\text{Ag/AgCl}}$  for 10 s. The deposition time was examined from 2 to 60 s, and the optimum activity was obtained for 10 s deposition. Then the deposition for 10 s was used hereafter. There are no specific redox peaks as much as general cyclic voltammograms of Ta-based catalysts,<sup>5–8</sup> while Pt catalysts have several redox peaks for the absorption/desorption of proton and formation/decomposition of surface oxide layer. However, a small decrease of the charge in an electrical double layer was observed after  $\text{H}_2$  treatment especially for long time treatment. The aggregation of CB particle was found with treatment for long time as discussed in section 3.4. The ionomer layer is thus considered to change the structure with the heat treatment, for example covering over the catalyst surface, and this change decreased the practical surface area. The decrease in charge in an electrical double layer is due to the decrease in surface area with the removal of organic impurities. Figures 3b,c display

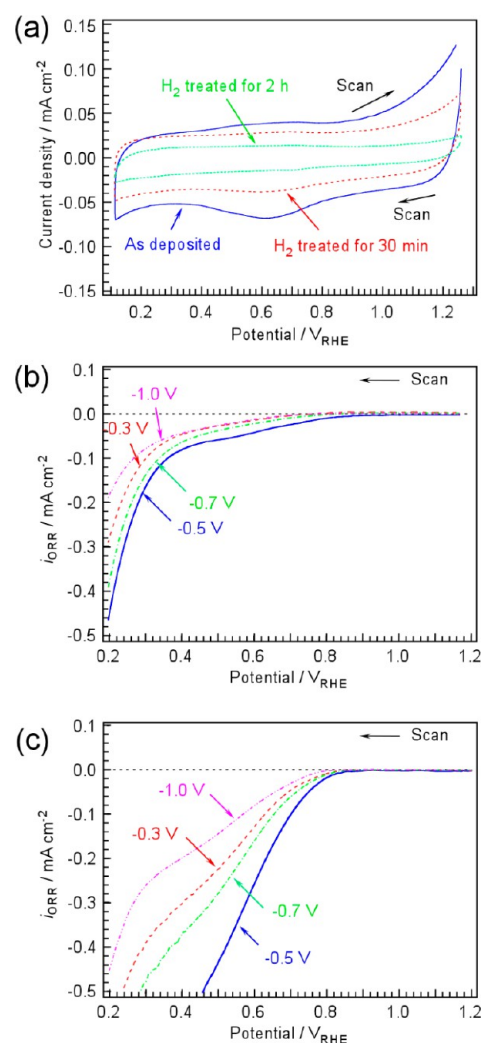


**Figure 3.** (a) Cyclic voltammograms of the  $\text{TaO}_x$  catalysts deposited on CB (Vulcan-XC72) at  $-0.5 V_{\text{Ag/AgCl}}$  for 10 s before and after  $\text{H}_2$  treatment for 30 min and 2 h. The potential was cycled with a scan rate of  $5 \text{ mV s}^{-1}$  under an Ar-saturated atmosphere. (b) Linear sweep voltammograms of the  $\text{TaO}_x$  catalysts electrodeposited on CB at  $-1.0$ ,  $-0.7$ ,  $-0.5$ ,  $-0.3 V_{\text{Ag/AgCl}}$  and the rest potential (without an applied potential) for 10 s. (c) Linear sweep voltammograms of the  $\text{TaO}_x$  catalysts treated under  $\text{H}_2$  at 523 K for 30 min after electrodeposition. All electrochemical measurements were performed in a  $0.1 \text{ M H}_2\text{SO}_4$  aqueous electrolyte saturated by Ar or  $\text{O}_2$  atmospheres at 298 K. The  $i_{\text{ORR}}$  indicates the difference between the current density measured under  $\text{O}_2$ -saturated and that under an Ar-saturated atmosphere, regarded as real catalytic activities for the ORR. The potential was cathodically swept with a scan rate of  $5 \text{ mV s}^{-1}$ .

voltammograms for the  $\text{TaO}_x$  catalysts which were electrodeposited on the CB electrodes under various potentials, including at rest,  $-0.3$ ,  $-0.5$ ,  $-0.7$ , and  $-1.0 V_{\text{Ag/AgCl}}$  before (b) and after (c) the  $\text{H}_2$  treatment at 523 K for 30 min. The current density,  $i_{\text{ORR}}$ , on the vertical axis in Figures 3b,c indicates the difference in the current density measured between the  $\text{O}_2$ -saturated and the Ar-saturated solution. As a blank test, the CB electrode just after immersion in the Ta plating solution for 10 s without an applied potential (at rest potential) seemed to show the catalytic properties of the carbon black itself with an onset potential of around  $0.45 V_{\text{RHE}}$  for the ORR, as represented in Figure 3b. Meanwhile, the  $\text{TaO}_x$  catalysts electrodeposited on the CB electrodes by the applied potentials

**Table 1.** Loading Amounts of Electrodeposited Ta onto CB Electrodes at Various Deposition Potentials<sup>a</sup>

applied potential ( $V_{\text{Ag/AgCl}}$ )	rest	−0.1	−0.3	−0.5	−0.7	−1.0
loading amounts ( $\text{mg Ta cm}^{-2}$ )	<0.0001	0.004	0.013	0.016	0.014	0.007

<sup>a</sup>The amounts of electrodeposited Ta were determined by ICP-AES.

showed ORR activity from much higher onset potentials. Among the as-electrodeposited catalysts, the  $\text{TaO}_x$  catalysts deposited at  $-0.5 V_{\text{Ag/AgCl}}$  for 10 s showed the largest ORR current with an onset potential of  $0.87 V_{\text{RHE}}$  (for  $2 \mu\text{A cm}^{-2}$ ). However, it still displayed low ORR current density for a potential of  $0.6\text{--}0.7 V_{\text{RHE}}$ , which is a reasonable voltage output range for PEFCs.<sup>32</sup> The  $\text{H}_2$  treatment was thus applied to the electrodeposited  $\text{TaO}_x$  electrodes at 523 K for 30 min. After the  $\text{H}_2$  treatment, the ORR current for all catalysts was considerably increased, as shown in Figure 3c. Furthermore, the current order of the respective  $\text{TaO}_x$  catalysts for the ORR followed to same trend with that before the  $\text{H}_2$  treatment. Under the present experimental conditions, the applied potential of  $-0.5 V_{\text{Ag/AgCl}}$  led to the highest catalytic activity, while the potential of  $-1.0 V_{\text{Ag/AgCl}}$  resulted in the lowest current. The  $\text{TaO}_x$  catalysts electrodeposited at  $-0.5 V_{\text{Ag/AgCl}}$  for 10 s followed by a  $\text{H}_2$  treatment exhibited an onset potential of  $0.92 V_{\text{RHE}}$  (for  $2 \mu\text{A cm}^{-2}$ ).

Basically, the properties of the  $\text{TaO}_x$  catalysts prepared by electrodeposition should be greatly influenced by the loading amounts and particle size of the Ta species. To explain the reasons why the catalysts prepared at  $-0.5 V_{\text{Ag/AgCl}}$  showed the best performance, the loading amounts of Ta species were estimated by ICP-AES. The results for six different  $\text{TaO}_x$ -electrodeposited electrodes are summarized in Table 1. For example, the catalyst deposited at  $-0.5 V_{\text{Ag/AgCl}}$  had  $0.016 \text{ mg cm}^{-2}$  of Ta, indicating that the weight ratio of Ta/CB was 3.2 wt % because of the CB amount of  $0.5 \text{ mg cm}^{-2}$ . The Ta loading on the CB electrodes deposited at the rest potential and at  $-0.1 V_{\text{Ag/AgCl}}$  was additionally measured to verify the dependence of the applied potentials on the electrodeposited amounts. The CB electrode prepared at the rest potential had almost negligible Ta loading. Accordingly, the activity of the catalyst prepared at the rest potential in Figure 3b is the same as for the CB electrode. Although more Ta species can be deposited on the CB electrode at a more negative potential, the loading amount of Ta under our deposition conditions was maximized at an applied potential of  $-0.5 V_{\text{Ag/AgCl}}$  and continuously decreased down to  $-1.0 V_{\text{Ag/AgCl}}$ . This is mainly because the reduction of Ta species competes with  $\text{H}_2$  evolution from HCl (eq 1) during electrodeposition. In practical terms, if  $\text{Ta}(\text{OC}_2\text{H}_5)_5$  was directly used instead of  $\text{TaCl}_5$ , the properties of the deposited catalysts would be obviously different from that in the present paper, and the presence of HCl plays a role in the electrodeposition. The competition between reduction of  $\text{Ta(V)}$  and reduction of  $\text{H}^+$  is clearly expressed in Figure 2. Accordingly, the loading amounts of electrodeposited Ta depending on the applied deposition potential were reflected in the ORR activity, and the  $\text{TaO}_x$  electrode prepared at  $-0.5 V_{\text{Ag/AgCl}}$  with the largest loading amounts resulted in the best ORR performance.

**3.3. Morphology and Size of  $\text{TaO}_x$  Nanoparticles Electrodeposited on CB.** Physical analyses were carried out to identify the reasons why the  $\text{TaO}_x$  catalysts fabricated by electrodeposition show high ORR activity. First, the surface morphology of the  $\text{TaO}_x$ -electrodeposited electrode, which was prepared by applying a potential of  $-0.5 V_{\text{Ag/AgCl}}$  to the Vulcan

CB electrode for 10 s and subsequently treatment under pure  $\text{H}_2$  gas at 523 K for 30 min, was established by STEM analysis, as visualized in Figure 4a. The much brighter small particles

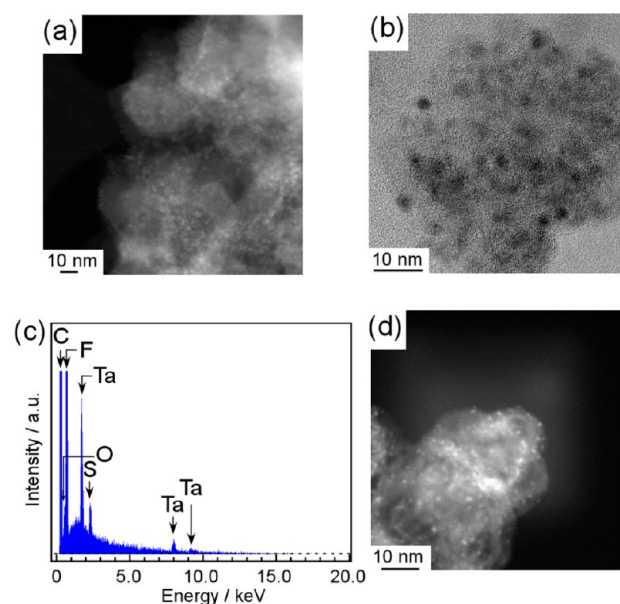


**Figure 4.** STEM (a) and TEM (b) images of the nanoscale  $\text{TaO}_x$  particles deposited on CB (Vulcan-XC72). (c) EDS results induced on the  $\text{TaO}_x$  electrodeposited electrode. (d) The STEM image shows  $\text{TaO}_x$  nanoparticles deposited on CB, Ketjen Black.

considered to be  $\text{TaO}_x$  particles with a size of a few nanometers were very uniformly distributed on the surface of the CB (Vulcan XC-72) with a diameter of 30–40 nm. EDS analysis was performed for the  $\text{TaO}_x$ -electrodeposited electrode. In addition to the plan-view STEM image, Figure 4b shows a TEM image of the  $\text{TaO}_x$  catalysts deposited on the CB measured to exactly confirm the particle size. Electrodeposited  $\text{TaO}_x$  particles seen as black spots were formed with an average 2–3 nm size under the optimized deposition conditions. The EDS spectrum in Figure 4c demonstrates that the electrode is made only of deposited Ta species and C, F, S, and O elements as components of the bare electrode, CB, and the Nafion ionomer. Furthermore, the  $\text{TaO}_x$  electrocatalysts deposited onto the Ketjen Black CB electrode under the same deposition conditions as used on the Vulcan CB were observed by STEM, as displayed in Figure 4d. The ORR properties of the  $\text{TaO}_x$  nanoparticles on Ketjen Black will be described in the following section. This STEM image illustrates that the smallest white particles were homogeneously dispersed onto the ball-like gray CB, and they were formed with much smaller average 1–2 nm size than that on the Vulcan CB. The competitive evolution of hydrogen generated from the dissolution of  $\text{TaCl}_5$  in ethanol during electrodeposition of Ta species might have allowed the deposits to form very small nanoparticles and to yield high dispersion on the two CB materials.<sup>20,46</sup> These outcomes suggested that the highly dispersive nanoparticle  $\text{TaO}_x$  catalysts could be prepared by an electrodeposition method and that

these optimized electrode structures resulted in excellent ORR performance originating from lots of efficient active sites.

**3.4. ORR Properties of Electrodeposited TaO<sub>x</sub> Catalysts Depending on Heat Treatment.** The effect of heat treatment on the ORR introduced to modify the surface conditions of the TaO<sub>x</sub>-electrodeposited electrodes was investigated by applying various heating environments. Figure 5 displays voltammograms of the TaO<sub>x</sub> catalysts electro-

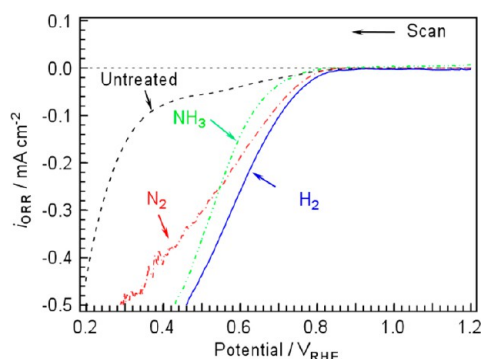


**Figure 5.** Linear sweep voltammograms of the TaO<sub>x</sub> catalysts deposited on CB (Vulcan-XC72) at a potential of  $-0.5 \text{ V}_{\text{Ag}/\text{AgCl}}$  for 10 s with heat treatment under NH<sub>3</sub>, N<sub>2</sub>, and H<sub>2</sub> flow at 1123 K (1 h), 523 K (0.5 h), and 523 K (0.5 h), respectively. All electrochemical measurements were performed in a 0.1 M H<sub>2</sub>SO<sub>4</sub> aqueous electrolyte saturated by Ar or O<sub>2</sub> atmospheres at 298 K. The  $i_{\text{ORR}}$  indicates the difference between current density measured under an O<sub>2</sub>-saturated and under an Ar-saturated atmosphere, regarded as real catalytic activities for the ORR. The potential was cathodically swept with a rate of  $5 \text{ mV s}^{-1}$ .

deposited at  $-0.5 \text{ V}_{\text{Ag}/\text{AgCl}}$  for 10 s onto the bare CB electrodes before and after treatment under different gases such as NH<sub>3</sub>, N<sub>2</sub>, and H<sub>2</sub>.

In Figure 5, the treatment under NH<sub>3</sub> gas at 1123 K for 1 h was specially applied to the TaO<sub>x</sub> catalysts electrodeposited on the bare PEG-bonded CB electrode instead of the Nafion ionomer.<sup>11–13</sup> The bare PEG-bonded CB electrode was prepared by spraying the CB slurry mixed with poly(ethylene glycol) (PEG) as a binder instead of a Nafion solution and by using the same composition ratio and loading level with the bare CB electrode. This was selected to prevent the release of toxic fluorine from the Nafion structure during the treatment at 1123 K. The NH<sub>3</sub> treatment was performed to form Ta<sub>3</sub>N<sub>5</sub>, which may exhibit higher ORR activity. The Ta-based catalysts after treatment by heating under NH<sub>3</sub> were found to be Ta<sub>3</sub>N<sub>5</sub> with an average particle size of 6 nm from the XRD patterns, as shown in Figure 6. Also, the TEM image in Figure 7 indicates that uniform Ta<sub>3</sub>N<sub>5</sub> particles with sizes of several nanometers are dispersed on the CB surfaces. The catalysts showed increased catalytic activity with an onset potential of  $0.81 \text{ V}_{\text{RHE}}$  (for  $2 \mu\text{A cm}^{-2}$ ) for the ORR after treatment, as indicated in Figure 5. The nitridation by NH<sub>3</sub> might have been expected to improve the electroconductivity of the Ta species, and it actually enhanced the ORR activity for the catalysts. However, this was not the most effective treatment for the electrodeposited TaO<sub>x</sub> catalysts.

Next, heat treatments were performed in N<sub>2</sub> or H<sub>2</sub> at 523 K for 30 min, as indicated in Figure 5. In the case of N<sub>2</sub> or H<sub>2</sub> treatment, no inherent XRD peaks for the TaO<sub>x</sub> catalysts were observed, and the Ta species were considered to be amorphous phases, in contrast to the NH<sub>3</sub>-treated catalysts. It is obvious

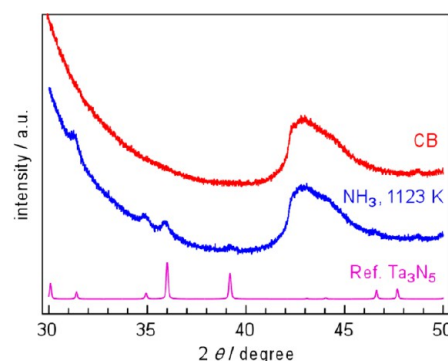


**Figure 6.** XRD patterns for the electrodeposited TaO<sub>x</sub> on CB (Vulcan-XC72) after NH<sub>3</sub> treatment at 1123 K for 1 h. The substrate was PEG-bonded Vulcan CB electrode as shown in the top trace. The bottom trace shows the Ta<sub>3</sub>N<sub>5</sub> reference data.

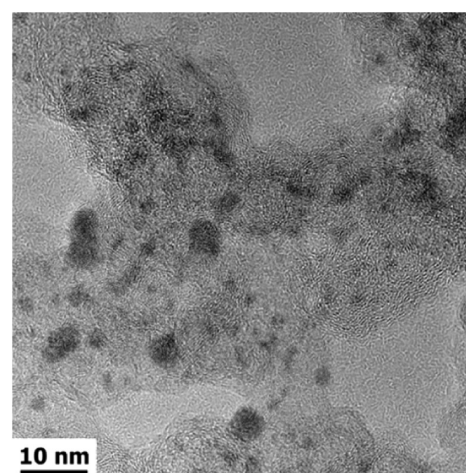


**Figure 7.** TEM image of the electrodeposited TaO<sub>x</sub> on CB (Vulcan-XC72) after NH<sub>3</sub> treatment at 1123 K for 1 h. Ta species assigned to Ta<sub>3</sub>N<sub>5</sub> as shown in Figure 6 were observed to be partially aggregated several nanometers sized particles.

that both treatments had a positive influence on ORR performance when compared to that of the untreated TaO<sub>x</sub> catalysts. Though the treatment under N<sub>2</sub> increased the catalytic activity with an onset potential of  $0.84 \text{ V}_{\text{RHE}}$  (for  $2 \mu\text{A cm}^{-2}$ ) for the ORR, it was not sufficiently large to improve the activity as much as that under the reducing atmosphere of H<sub>2</sub> gas. As a result, the best modification on the surface of the TaO<sub>x</sub>-electrodeposited electrode was realized under H<sub>2</sub> treatment for excellent ORR performance. The oxidation state of Ta was not changed by the heat treatment as discussed in the next section (Figure 10), and organic residues were removed from the surface by the treatment. The difference between H<sub>2</sub> and N<sub>2</sub> for the treatment has now been cleared, and the mechanism should be clarified with further examination. Many researchers have reported that heat treatment plays an important role in improving ORR activity and stability.<sup>9,33–35</sup> Cheng et al. indicated that heat treatment in H<sub>2</sub> at 673 K for 1 h improved the ORR activity and stability of an RuSe electrocatalyst.<sup>35</sup> They also mentioned that the positive effects of H<sub>2</sub> treatment at low temperature were found to be removal of residues after synthesis, crystallization, reduction of oxygen groups on the support surface, and the formation of catalytic sites. Based on this insight into the effects of H<sub>2</sub> treatment, excellent ORR performance for the H<sub>2</sub>-treated TaO<sub>x</sub> catalysts might be



expected under our experiment environment, electrodeposition under a nonaqueous plating bath, and a material that is easily oxidized at room temperature. Additional explanations of the effects of  $\text{H}_2$  treatment will be discussed with regard to the XPS analysis.

Based on its superior performance, the  $\text{H}_2$  treatment was optimized by altering the heating temperature and time period. Figure 8a shows voltammograms recorded for  $\text{TaO}_x$  catalysts

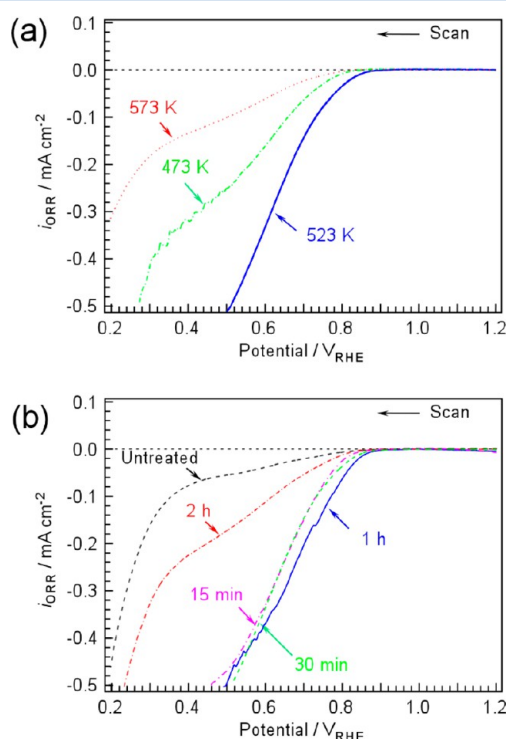


**Figure 8.** ORR activities of the  $\text{TaO}_x$  catalysts on CB (Vulcan-XC72) electrodes as a function of the  $\text{H}_2$  treatment conditions. The graphs show voltammograms for the  $\text{TaO}_x$  catalysts deposited at a potential of  $-0.5 \text{ V}_{\text{Ag}/\text{AgCl}}$  for 10 s and followed by  $\text{H}_2$  treatment under different heating temperatures of 573, 523, and 473 K for 30 min (a) and under various heating times such as untreated, 15 min, 30 min, 1 h, and 2 h at 523 K (b). The potential was cathodically swept in 0.1 M  $\text{H}_2\text{SO}_4$  aqueous electrolyte with a scan rate of  $5 \text{ mV s}^{-1}$  under  $\text{Ar}$ -saturated and  $\text{O}_2$ -saturated atmospheres at 298 K.

fabricated at  $-0.5 \text{ V}_{\text{Ag}/\text{AgCl}}$  for 10 s and then treated in pure  $\text{H}_2$  by heating at 473, 523, and 573 K for 30 min. The range of desired temperatures was determined to be lower than 600 K, which is the melting point for the tetrafluoroethylene (PTFE) backbone of Nafion which was used as a binder for the bare CB electrodes. As displayed in Figure 8a, the catalysts treated at 523 K for 30 min presented the optimum temperature for the best ORR activity. Actually, the Nafion ionomer structure is expected to break up around 573 K according to thermal gravimetric analysis (TGA).<sup>36,37</sup> Figure 8b indicates the influence of the time period for  $\text{H}_2$  treatment at 523 K, including 15, 30, 60, and 120 min, on the ORR activity. The best ORR performance converged on the treatment at 523 K for 60 min. It was however revealed that the performance of  $\text{TaO}_x$  catalysts  $\text{H}_2$ -treated from 15 to 60 min was not distinctly different, even if it was tried several times. Moreover, a long treatment of 2 h decreased the ORR activity. The SEM images in Figure 9 present the different surface structures for the  $\text{H}_2$ -treated electrodes at 523 K for 30 and 120 min. The long treatment time of 2 h led to aggregation of the CB powder, and the undesirable change in the macroscopic structure gave rise to a negative effect on the ORR activity. The  $\text{H}_2$  treatment did not change the oxidation state of Ta as discussed in the next section, so that the decrease of ORR current should be explained by the structural change of ionomer layer which leads the aggregation of CB powders for long time treatment. This change contributes the decrease of electric double layer capacitance (surface area) as discussed in section 3.2. The optimum heating temperature and time for improving ORR performance commonly rely on the properties of individual catalysts and the electrode structure. To conclude, the electrodeposited  $\text{TaO}_x$  catalysts after  $\text{H}_2$  treatment at 523 K for 1 h exhibited the most improved ORR performance based on the surface morphology of the highly dispersed nanoparticles as confirmed from (S)TEM images.

**3.5. XPS Analysis of the Electrodeposited  $\text{TaO}_x$  Electrodes.** In our previous communication, we reported that the surface phase of electrodeposited  $\text{TaO}_x$  catalysts turned out to be an oxide form, such as  $\text{Ta}_2\text{O}_5$  but not metallic Ta, according to the double splitting peak of Ta  $4f_{7/2}$  over the assigned  $\text{Ta}_2\text{O}_5$  position.<sup>26</sup> In this study, a more detailed investigation of the electrodeposited Ta species was performed by XPS measurements to identify the reasons why the  $\text{H}_2$ -treated catalysts prepared by electrodeposition showed improved ORR activity and a suitable onset potential for the

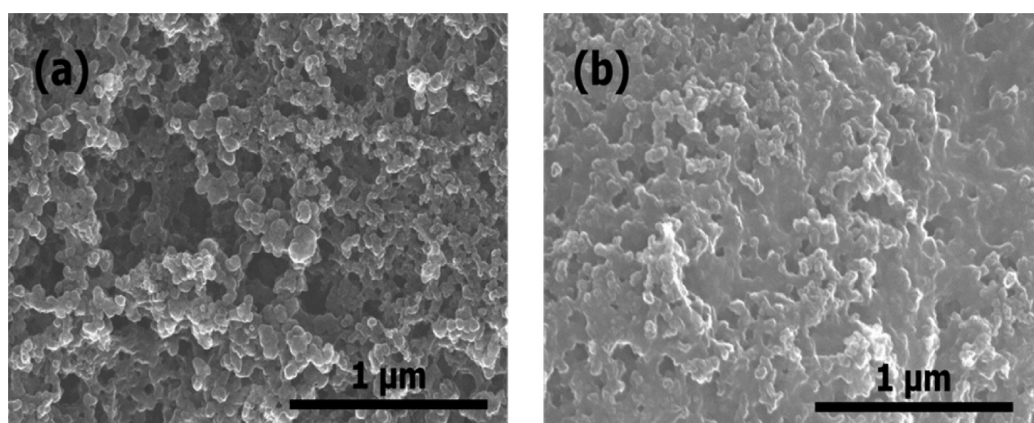


**Figure 9.** SEM images of the  $\text{TaO}_x$  catalysts deposited on CB (Vulcan-XC72) electrode after  $\text{H}_2$  treatment at 523 K for 30 min (a) and 2 h (b).

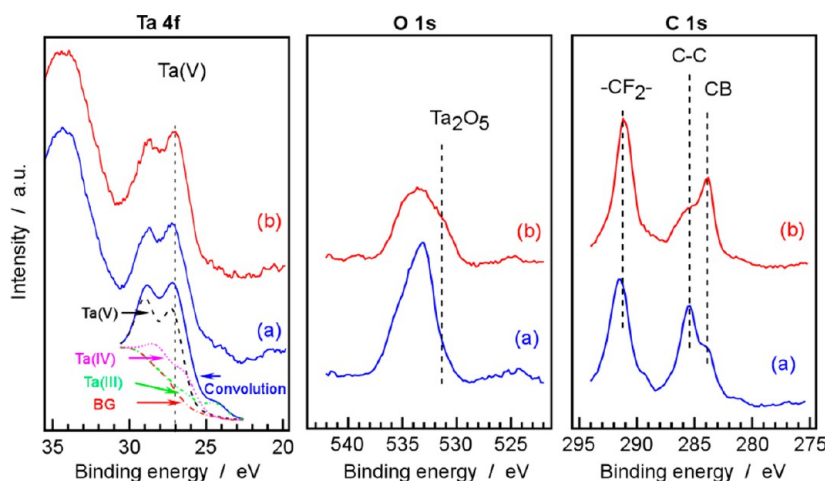


**Figure 10.** Narrow scanned XPS spectra for Ta 4f, O 1s, and C 1s of electrodeposited TaO<sub>x</sub> catalysts on CB (Vulcan-XC72) before (a) and after (b) heat treatment (H<sub>2</sub>, 523 K, 30 min). The narrow scan of the Ta 4f XPS spectra was measured for the electrodes after Ar<sup>+</sup> bombardment for 90 s.

ORR. Figure 10 displays Ta 4f, O 1s, and C 1s XPS spectra for the electrodeposited TaO<sub>x</sub> catalysts before and after H<sub>2</sub> treatment at 523 K for 30 min. In particular, the narrow scans of the Ta 4f XPS spectra were measured for the electrodes after Ar<sup>+</sup> ion bombardment at an acceleration voltage of 500 eV for 90 s to observe the interior chemical states of the TaO<sub>x</sub> nanoparticles.

As discussed in the previous paper, the Ta 4f spectra both before and after the H<sub>2</sub> treatment pointed to the undeniable fact that the Ta species on CB were deposited in an oxide form and not in a metallic state. There was no distinguishable difference in the Ta 4f spectra obtained before and after the H<sub>2</sub> treatment. Moreover, they did not show a pair of typical double split peaks corresponding to the Ta<sub>2</sub>O<sub>5</sub> species. The broad Ta 4f spectrum for the untreated TaO<sub>x</sub> electrode was deconvoluted into three oxidation states, labeled Ta<sub>2</sub>O<sub>5</sub>(Ta(V)), TaO<sub>2</sub>(Ta(IV)), and TaO<sub>2-x</sub> ( $x \leq 1$ ) (Ta(III)), consistent with previous reference data.<sup>22,31,38–41</sup> The peak positions of Ta 4f<sub>7/2</sub> for the three components were assigned based on differences between the binding energies of 5.55, 4.80, and 2.76 eV and the value of 21.6 eV for metallic Ta 4f<sub>7/2</sub>. The spin–orbit doublet separation at  $1.8 \pm 0.1$  eV for all Ta 4f states and a fwhm of 1.5 eV for Ta<sub>2</sub>O<sub>5</sub> and 1.65 eV for TaO<sub>2</sub> and TaO<sub>2-x</sub> were maintained for the best curve fitting of the electrodeposited TaO<sub>x</sub> catalysts. The peak position at 34 eV in the Ta 4f spectrum was assigned to the binding energy of F 2s from the Nafion ionomer.

Based on the deconvolution, the Ta 4f spectrum consisted of 63% Ta<sub>2</sub>O<sub>5</sub>, 25% TaO<sub>2</sub>, and 12% TaO<sub>2-x</sub> ( $x \leq 1$ ). This clearly indicates that the most abundant state of the electrodeposited TaO<sub>x</sub> species was Ta(V). The existence of Ta(IV) and Ta(III) species was considered, from the reduction of the Ta(V) ethoxide species, to be deposited on the CB during the electrodeposition. These might be easily reoxidized to Ta(V) by air or H<sub>2</sub>O impurity after electrodeposition. Thus, the electrodeposited TaO<sub>x</sub> particles reflect this composition ratio of the oxidation states. It has been reported that suboxide nanoparticles such as TaO<sub>x</sub>, ZnO<sub>x</sub>, and TiO<sub>x</sub> have more enhanced electroconductivity than oxides with the highest oxidation state through the changed electronic conduction originating from the oxygen vacancy.<sup>42–44</sup> Moreover, pure Ta<sub>2</sub>O<sub>5</sub> in the bulk can hardly be expected to show catalytic activity as an electrocatalyst because it is an insulator. However,

it has been reported that Ta<sub>2</sub>O<sub>5</sub> nanoparticles with sizes of smaller than 8 nm have totally different electrical properties compared to the bulk; i.e., some conductivity can be expected for the nanoscale tantalum oxides because the donor density is very high for a ferroelectric layer in the Ta<sub>2</sub>O<sub>5</sub> nanoparticles.<sup>45</sup> On the basis of the above, it can be explained why highly dispersed TaO<sub>x</sub> nanoparticles with an average size of 2–3 nm prepared by electrodeposition display excellent catalytic activity for the ORR.

The O 1s and C 1s spectra before and after the H<sub>2</sub> treatment were compared to establish the effect of H<sub>2</sub> treatment on surface modification of the electrodes. In the O 1s spectra, shown in Figure 10, the intensity of the O 1s peak decreased after the treatment relative to that of the Ta peaks. This indicates that a part of the oxygen on Ta<sup>5+</sup> sites was removed by the hydrogen treatment. However, the O 1s peak contains signals from many types of O species, such as the ionomer and oxygen-containing terminals of CB, not just TaO<sub>x</sub>, so that the TaO<sub>x</sub> species seems not to be reduced. The most important finding from the XPS spectra was that the intensity of the organic C–C bonding positioned at the binding energy of 286 eV was significantly decreased after the H<sub>2</sub> treatment, based on the intensity of the C 1s peak at this energy. Concurrently, the relative intensity of the C 1s peak at 284 eV increased; this position corresponds to pure carbon black. This may be caused by the removal of adsorbed organic impurities that probably remained after electrodeposition, which means much larger TaO<sub>x</sub> nanoparticles are exposed on the surface of the electrode. The C 1s peak at 291 eV was assigned to F-bonded carbon, from the Nafion ionomer, and the H<sub>2</sub> treatment did not affect this peak. Overall, surface modification by the H<sub>2</sub> treatment, leading to more exposed active sites on the TaO<sub>x</sub>-electrodeposited electrode, resulted in improved ORR activity.

**3.6. Long-Term Stability of the Electrodeposited TaO<sub>x</sub> Catalysts.** The long-term stability of the TaO<sub>x</sub>-electrodeposited electrode was evaluated by an accelerated durability measurement. Figure 11 displays current retention at 0.60 V<sub>RHE</sub> of the typical ORR performance for the H<sub>2</sub>-treated TaO<sub>x</sub> catalysts during the accelerated durability test. For this test, linear sweep voltammetry in the range of 0.6–1.23 V<sub>RHE</sub> of the potential was repeated 1000 times with an accelerated scan rate of 50 mV s<sup>−1</sup> in a 0.1 M H<sub>2</sub>SO<sub>4</sub> aqueous solution under an O<sub>2</sub>-saturated atmosphere at 298 K. During the test, the typical



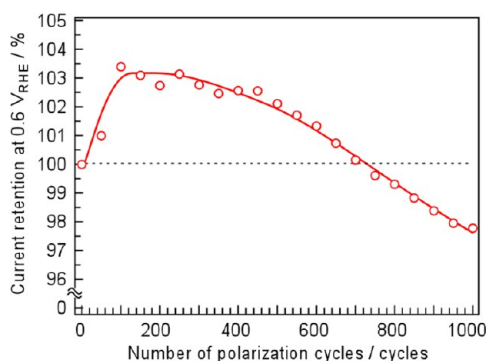


**Figure 11.** Current retention at  $0.60 V_{\text{RHE}}$  of typical ORR performance for the heat-treated  $\text{TaO}_x$  catalysts on the CB (Vulcan-XC72) electrode during the accelerated durability test for 1000 cycles. The accelerated polarization was swept between  $1.23$  to  $0.60 V_{\text{RHE}}$  at cathodic and anodic scan rates of  $50 \text{ mV s}^{-1}$  for 1000 cycles. The ORR activities for the current density at  $0.60 V_{\text{RHE}}$  were measured in the potential range of  $1.23$ – $0.20 V_{\text{RHE}}$  with a cathodic scan rate of  $5 \text{ mV s}^{-1}$  after every 50 accelerated cycles. All electrochemical measurements were performed in a  $0.1 \text{ M H}_2\text{SO}_4$  aqueous solution under an  $\text{O}_2$ -saturated atmosphere at  $298 \text{ K}$ .

ORR performance was also recorded at a potential in the range of  $0.2$ – $1.23 V_{\text{RHE}}$  with a scan rate of  $5 \text{ mV s}^{-1}$  per 50 accelerated cycles. The retained current at  $0.60 V_{\text{RHE}}$  was calculated from the ORR cathodic current density. As shown in Figure 11, there is no obvious current degradation for the ORR performance during the durability test. The electrodeposited  $\text{TaO}_x$  catalysts retained 97.8% of the current density at the designated potential of  $0.6 V_{\text{RHE}}$  for the ORR after 1000 cycles. This high retention clearly demonstrates that the  $\text{TaO}_x$  catalysts prepared by electrodeposition have sufficient durability in an acidic solution, in line with the expectation for chemically stable properties of oxides.

**3.7. ORR Performance of  $\text{TaO}_x$  Nanoparticles Electrodeposited on Different Carbon Blacks.** A different CB material, Ketjen Black (EC-600JD), with a large surface area was next examined. Figure 12 shows a comparison of polarization curves for ORR activities of the heat-treated  $\text{TaO}_x$  catalysts deposited on the Vulcan and Ketjen Black CB under the same deposition conditions. The surface areas were reported to be around  $300$  and  $1200 \text{ m}^2 \text{ g}^{-1}$  for Vulcan XC-72

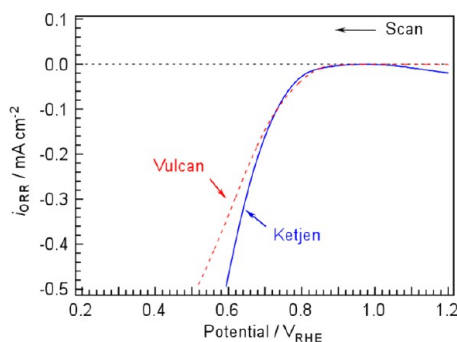


**Figure 12.** ORR activities for  $\text{TaO}_x$  catalysts electrodeposited on different kinds of carbon black. The graph indicates voltammograms of the  $\text{TaO}_x$  catalysts deposited on VulcanXC-72 and Ketjen Black EC-600JD at a potential of  $-0.5 V_{\text{Ag/AgCl}}$  for 10 s and followed by  $\text{H}_2$  treatment at  $523 \text{ K}$  for 30 min. The potential was cathodically swept in the  $0.1 \text{ M H}_2\text{SO}_4$  aqueous electrolyte at a scan rate of  $5 \text{ mV s}^{-1}$  under  $\text{Ar}$ -saturated and  $\text{O}_2$ -saturated atmospheres at  $298 \text{ K}$ .

and Ketjen Black (EC-600JD), respectively.<sup>47–49</sup> The Ta amounts loaded on the carbon electrode using Ketjen Black were measured by ICP-AES. The amount of deposited Ta on Ketjen Black was  $0.027 \text{ mg Ta cm}^{-2}$  while that on Vulcan was  $0.016 \text{ mg Ta cm}^{-2}$ . The onset potential of  $\text{TaO}_x$  catalysts of Ketjen Black for ORR was almost same to that of Vulcan CB, indicating similar  $\text{TaO}_x$  nanoparticles were formed on the CB surfaces. As shown in Figure 4d, uniform  $\text{TaO}_x$  nanoparticles were well-dispersed on Ketjen Black, similar to the corresponding distribution on Vulcan, even if larger amounts of Ta were loaded. The  $\text{TaO}_x$  catalysts loaded on Ketjen Black showed a higher cathodic current density for the ORR around  $0.6 V_{\text{RHE}}$ . The electrodeposited amounts of Ta on Ketjen Black was higher than that on Vulcan CB, though not in proportion to the surface area. The higher electrodeposited amounts resulted in the higher ORR current around  $0.6 V_{\text{RHE}}$ . It has been known that mesoporous carbon supports such as Ketjen Black and Black Pearl enable deposited electrocatalysts to be well-dispersed with their pore morphology facilitating mass transport.<sup>47–52</sup>

### 3.8. Comparison with Commercial Pt/CB Catalysts.

The ORR properties of the electrodeposited  $\text{TaO}_x$  catalysts on CB was compared with that of commercial Pt/CB catalysts. To form a Pt/CB catalyst slurry, commercial 20 wt % Pt/CB (EC-20-PTC, Electrochem, Inc., Pt on Vulcan XC-72R) was first mixed with Nafion solution in an IPA solvent. The composition ratio of the catalyst to the Nafion ionomer was 4:1. The well-dispersed slurry was sprayed on the bare carbon electrode by fixing the amount of Pt loading at  $0.025 \text{ mg Pt cm}^{-2}$ . The catalytic activity for the  $\text{TaO}_x$ -electrodeposited Vulcan CB electrode prepared at  $-0.5 V_{\text{Ag/AgCl}}$  for 10 s was compared and contrasted with that for the Pt/CB electrode. The activities were evaluated by conventional ORR measurements. Because of difficulty of fabrication of rotating disk electrode (RDE) with our electrocatalysts, we cannot evaluate kinetic current for ORR and the ORR property of the catalysts on carbon sheet was compared.

Figure 13 shows a comparison of the mass activities for the ORR between the electrodeposited  $\text{TaO}_x$  and commercial Pt/CB electrodes. The prepared Pt/CB electrode showed typical

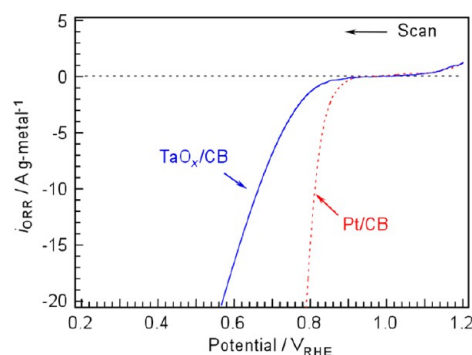


**Figure 13.** Comparison of mass activities for the ORR between the electrodeposited  $\text{TaO}_x$  on CB (Vulcan-XC72) and commercial Pt/CB catalysts. The vertical axis was corrected as the mass-specific current for the loading amounts of Ta or Pt. The potential was cathodically swept in the  $0.1 \text{ M H}_2\text{SO}_4$  aqueous electrolyte at a scan rate of  $5 \text{ mV s}^{-1}$  under  $\text{Ar}$ -saturated and  $\text{O}_2$ -saturated atmospheres at  $298 \text{ K}$ . The  $i_{\text{ORR}}$  indicates the difference in ORR activities under  $\text{O}_2$ -saturated and  $\text{Ar}$ -saturated atmospheres. The loading amounts of Ta and Pt were  $0.016$  and  $0.025 \text{ mg cm}^{-2}$ .

ORR activity and an onset potential of ca. 0.97 V<sub>RHE</sub> for the Pt catalysts. From the onset potential viewpoint, the TaO<sub>x</sub>/CB catalysts by electrodeposition obviously had a higher overpotential for the ORR than for the Pt/CB catalysts. However, the difference in the onset potential between the Pt/CB and TaO<sub>x</sub>/CB catalysts was only ca. 0.05 V. In the present current region below 20 A g metal<sup>-1</sup>, the difference of over potential between TaO<sub>x</sub>/CB and Pt/CB is 0.05–0.2 V. This means that the electrodeposited TaO<sub>x</sub> exhibited a high utilization of catalysts for the ORR activity. Although the catalytic performance for the electrodeposited TaO<sub>x</sub>/CB approached that for the Pt/CB, the Ta loading was significantly limited for application in fuel cells at present. Therefore, there remains a future challenge to improve the performance of the TaO<sub>x</sub> catalysts accompanied by high loading.

One problem for the oxide/nitride catalysts of group IV and V transition metals is the two-electron reduction to H<sub>2</sub>O<sub>2</sub>, which is more obvious than for the Pt catalysts. In the present method, it was hard to prepare a rotating ring-disk electrode (RRDE) because of the nonaqueous electrodeposition bath wherein a mirror-finished GC electrode cannot hold the CB particles. A significant fraction of H<sub>2</sub>O<sub>2</sub> was detected for the oxide/nitride catalysts of group IV and V transition metals.<sup>10,53</sup> However, an ORR current was observed at much above 0.7 V<sub>RHE</sub>, which is the equilibrium potential for two-electron reduction, indicating that this catalyst has obvious activity for a four-electron reduction to H<sub>2</sub>O.

#### 4. CONCLUSIONS

TaO<sub>x</sub> nanoparticles for cathode electrocatalysts of PEFCs were successfully prepared by cathodic deposition from an ethanol-based Ta plating solution at room temperature. According to the fundamental polarization curves of the Ta(V) complexes in the deposition solution, the catalytic performance of the TaO<sub>x</sub> particles electrodeposited on the CB electrode was maximized under an applied potential of −0.5 V<sub>Ag/AgCl</sub> for 10 s. This was mainly attributed to the amounts of Ta loading relied on the deposition potential. Moreover, electrodeposited TaO<sub>x</sub> species were formed with a highly uniform distribution and an average nanoparticle size of 2–3 nm on the surface of the CB supports, according to electron microscope analysis. Nanosize control of the TaO<sub>x</sub> particles was achieved by adjusting the electrodeposition conditions used, such as the applied potential, time of deposition, and the competing reduction species, H<sup>+</sup>, in our experiments.

In fact, heat treatment of the TaO<sub>x</sub> electrode after electrodeposition under various flowing gases including NH<sub>3</sub>, N<sub>2</sub>, and H<sub>2</sub> at 523 K for 30 min showed a positive influence on catalytic activity for the ORR. By optimizing the heat treatment conditions, TaO<sub>x</sub> nanoparticles heated under H<sub>2</sub> at 523 K for 60 min showed the best catalytic activity with an onset potential of 0.93 V<sub>RHE</sub> (for 2 μA cm<sup>-2</sup>) for the ORR. The H<sub>2</sub> treatment was a necessary step for introducing active catalytic sites on the surface of the TaO<sub>x</sub>-electrodeposited electrode by removing the residues of the remaining organic solvent after the electrodeposition. Chemical identification of the electrodeposited material on the CB indicated that it was tantalum oxide, TaO<sub>x</sub>, which effectively promoted electroconductivity mainly due to the presence of mixed TaO<sub>2</sub> and Ta<sub>2</sub>O<sub>5</sub>, according to XPS analysis.

The electrodeposited TaO<sub>x</sub> nanoparticles showed very stable properties under an acidic solution as indicated by accelerated durability testing. The TaO<sub>x</sub> catalysts electrodeposited on CB

showed high catalytic utilization for the ORR, comparable to that using commercial Pt/C catalysts, though the improvement of performance depended on high loading of the electrodeposited Ta. Therefore, the TaO<sub>x</sub> nanoparticles obtained by electrodeposition show very good potential as new oxygen reduction electrocatalysts for PEFCs.

#### AUTHOR INFORMATION

##### Corresponding Author

\*E-mail: kdomen@chemsys.t.u-tokyo.ac.jp (K.D.).

##### Notes

The authors declare no competing financial interest.

#### ACKNOWLEDGMENTS

This work was supported in part by the Funding Program for World-Leading Innovative R&D on Science and Technology (FIRST) of the Cabinet Office of Japan and “Elements Strategy Initiative for Catalysts & Batteries (ESICB)” supported by the MEXT program “Elements Strategy Initiative to Form Core Research Center” (since 2012) of the Ministry of Education, Culture, Sports, Science and Technology (MEXT), Japan. This work also contributes the international exchange program of the A3 Foresight Program of the Japan Society for the Promotion of Science (JSPS). One of authors, Seo, appreciates the support of the Global Centers of Excellence (GCOE) Program of JSPS for her work at the University of Tokyo.

#### REFERENCES

- (1) Lefevre, M.; Proietti, E.; Jaouen, F.; Dodelet, J.-P. Iron-Based Catalysts with Improved Oxygen Reduction Activity in Polymer Electrolyte Fuel Cells. *Science* **2009**, *324*, 71–74.
- (2) Bezerra, C. W. B.; Zhang, L.; Lee, K. A Review of Fe-N/C and Co-N/C Catalysts for the Oxygen Reduction Reaction. *Electrochim. Acta* **2008**, *53*, 4937–4951.
- (3) Yin, F.; Takanabe, K.; Kubota, J.; Domen, K. Improved Catalytic Performance of Nitride Co-Ti and Fe-Ti Catalysts for Oxygen Reduction as Non-noble Metal Cathodes in Acidic Media. *Electrochem. Commun.* **2010**, *12*, 1177–1179.
- (4) Rabis, A.; Rodriguez, P.; Schmidt, T. J. Electrocatalysis for Polymer Electrolyte Fuel Cells: Recent Achievements and Future Challenges. *ACS Catal.* **2012**, *2*, 864–890.
- (5) Ishihara, A.; Lee, K.; Doi, S.; Mitsushima, S.; Kamiya, N.; Hara, M.; Domen, K.; Fukuda, K.; Ota, K. Tantalum Oxynitride for a Novel Cathode of PEFC. *Electrochem. Solid-State Lett.* **2005**, *8*, A201–A203.
- (6) Ishihara, A.; Shibata, Y.; Mitsushima, S.; Ota, K. Partially Oxidized Tantalum Carbonitrides as a New Nonplatinum Cathode for PEFC. *J. Electrochem. Soc.* **2008**, *155*, B400–B406.
- (7) Ishihara, A.; Tamura, M.; Matsuzawa, K.; Mitsushima, S.; Ota, K. Tantalum Oxide-Based Compounds as New Non-noble Cathodes for Polymer Electrolyte Fuel Cell. *Electrochim. Acta* **2010**, *55*, 7581–7589.
- (8) Oh, T.; Kim, J. Y.; Shin, Y.; Engelhard, M.; Weil, K. S. Effects of Tungsten Oxide Addition on the Electrochemical Performance of Nanoscale Tantalum Oxide-Based Electrocatalysts for Proton Exchange Membrane (PEM) Fuel Cells. *J. Power Sources* **2011**, *196*, 6099–6103.
- (9) Bezerra, C. W. B.; Zhang, L.; Liu, H.; Lee, K.; Marques, A. L. B.; Marques, E. P.; Wang, H.; Zhang, J. A Review of Heat-treatment Effects on Activity and Stability of PEM Fuel Cell Catalysts for Oxygen Reduction Reaction. *J. Power Sources* **2007**, *173*, 891–908.
- (10) Takagaki, A.; Takahashi, Y.; Yin, F.; Takanabe, K.; Kubota, J.; Domen, K. Highly Dispersed Niobium Catalyst on Carbon Black by Polymerized Complex Method as PEFC Cathode Catalyst. *J. Electrochem. Soc.* **2009**, *156*, B811–B815.
- (11) Ohnishi, R.; Katayama, M.; Takanabe, K.; Kubota, J.; Domen, K. Niobium-Based Catalysts Prepared by Reactive Radio-frequency Magnetron Sputtering and Arc Plasma Methods as Non-noble Metal

Cathode Catalysts for Polymer Electrolyte Fuel Cells. *Electrochim. Acta* **2010**, *55*, 5393–5400.

(12) Chen, J.; Takanabe, K.; Ohnishi, R.; Li, D.; Okada, S.; Hatasawa, H.; Morioka, H.; Antonietti, M.; Kubota, J.; Domen, K. Nano-sized TiN on Carbon Black as an Efficient Electrocatalyst for the Oxygen Reduction Reaction Prepared Using an mpg-C<sub>3</sub>N<sub>4</sub> Template. *Chem. Commun.* **2010**, *46*, 7492–7494.

(13) Isogai, S.; Ohnishi, R.; Katayama, M.; Kubota, J.; Kim, D. Y.; Noda, S.; Cha, D.; Takanabe, K.; Domen, K. Composite of TiN Nanoparticles and Few-Walled Carbon Nanotubes and Its Application to the Electrocatalytic Oxygen Reduction Reaction. *Chem.—Asian J.* **2012**, *7*, 286–289.

(14) Takasu, Y.; Suzuki, M.; Yang, H. S.; Ohashi, T.; Sugimoto, W. Oxygen Reduction Characteristics of Several Valve Metal Oxide Electrodes in HClO<sub>4</sub> Solution. *Electrochim. Acta* **2010**, *55*, 8220–8229.

(15) Kim, J. Y.; Oh, T.; Shin, Y.; Bonnett, J. F.; Weil, K. S. A Novel Non-platinum Group Electrocatalyst for PEM Fuel Cell Application. *Int. J. Hydrogen Energy* **2011**, *36*, 4557–4564.

(16) Macagno, V. A.; Schultze, J. W. The Growth and Properties of Thin Oxide Layers on Tantalum Electrodes. *J. Electroanal. Chem.* **1984**, *180*, 157–170.

(17) Lee, J.; Seo, J.; Han, K.; Kim, H. Preparation of Low Pt Loading Electrodes on Nafion(Na<sup>+</sup>)-bonded Carbon Layer with Galvanostatic Pulses for PEMFC Application. *J. Power Sources* **2006**, *163*, 349–356.

(18) Tominaka, S.; Momma, T.; Osaka, T. Electrodeposited Pd-Co Catalyst for Direct Methanol Fuel Cell Electrodes: Preparation and Characterization. *Electrochim. Acta* **2008**, *53*, 4679–4686.

(19) Kim, H.; Subramanian, M. P.; Popov, B. N. Preparation of PEM Fuel Cell Electrodes Using Pulse Electrodeposition. *J. Power Sources* **2004**, *138*, 14–24.

(20) Paunovic, M.; Schlesinger, M. *Electrochemical Society Series, Fundamental of Electrochemical Deposition*; Wiley-Interscience Pub.: New York, 1998.

(21) Simka, W.; Puszzyk, D.; Nawrat, G. Electrodeposition of Metals from Non-aqueous Solutions. *Electrochim. Acta* **2009**, *54*, 5307–5319.

(22) Sata, S.; Awada, M. I.; El-Deaba, M. S.; Okajima, T.; Ohsaka, T. Hydrogen Spillover Phenomenon: Enhanced Reversible Hydrogen Adsorption/Desorption at Ta<sub>2</sub>O<sub>5</sub>-Coated Pt Electrode in Acidic Media. *Electrochim. Acta* **2010**, *55*, 3528–3536.

(23) Masud, J.; Alam, M. T.; Okajima, T.; Ohsaka, T. Catalytic Electrooxidation of Formaldehyde at Ta<sub>2</sub>O<sub>5</sub>-Modified Pt Electrodes. *Chem. Lett.* **2011**, *40*, 252–254.

(24) El Abedin, S. Z.; Welz-Biermann, U.; Endres, F. A Study on the Electrodeposition of Tantalum on NiTi Alloy in an Ionic Liquid and Corrosion Behavior of the Coated Alloy. *Electrochem. Commun.* **2005**, *7*, 941–946.

(25) El Abedin, S. Z.; Farag, H. K.; Moustafa, E. M.; Welz-Biermann, U.; Endres, F. Electroreduction of Tantalum Fluoride in a Room temperature Ionic Liquid at Variable Temperatures. *Phys. Chem. Chem. Phys.* **2005**, *7*, 2333–2339.

(26) Seo, J.; Cha, D.; Takanabe, K.; Kubota, J.; Domen, K. Highly-Dispersed Ta-Oxide Catalysts Prepared by Electrodeposition in a Non-aqueous Plating Bath for Polymer Electrolyte Fuel Cell Cathodes. *Chem. Commun.* **2012**, *48*, 9074–9076.

(27) Winter, M. The University of Sheffield and WebElements Ltd., UK, <http://www.webelements.com/tantalum/compounds.html>.

(28) Sata, S.; Okajima, T.; Kitamura, F.; Kaneda, K.; Ohsaka, T. Enhanced Hydrogen Adsorption/Desorption Characteristic of Ta<sub>2</sub>O<sub>5</sub>-coated Pt Electrode Prepared by Electrodeposition of Ta and the Subsequent Calcination. *Chem. Lett.* **2007**, *36*, 572–573.

(29) Bursten, B. E.; Green, M. R.; Katovic, V.; Kirk, J. R.; Lightner, D. Electrochemistry of Niobium(IV) and Tantalum(IV) Complexes: Ligand Additivity in d<sup>1</sup> Octahedral Complexes. *Inorg. Chem.* **1986**, *25*, 831–834.

(30) Skompska, M.; Vorotyntsev, M. A.; Goux, J.; Gendre, P. L.; Moise, C. Electrochemical Properties of Metallocene Hydroxo and Oxo Complexes of Ta(V):[Cp\*(CpR)TaOHCl]<sup>+</sup>Cl<sup>−</sup>, R = H, SiMe<sub>3</sub> or (CH<sub>2</sub>)<sub>3</sub>NC<sub>4</sub>H<sub>4</sub>, Cp\*(Cp(CH<sub>2</sub>)<sub>3</sub>NC<sub>4</sub>H<sub>4</sub>)TaOCl: Electrochemical Dep-

osition of Conducting Polymer Film with Incorporated Tantalocene Complexes. *Electrochim. Acta* **2008**, *53*, 3844–3853.

(31) Awaludin, Z.; Suzuki, M.; Masud, J.; Okajima, T.; Ohsaka, T. Enhanced Electrocatalysis of Oxygen Reduction on Pt-TaO<sub>x</sub>/GC. *J. Phys. Chem. C* **2011**, *115*, 25557–25567.

(32) Wang, Y.; Song, S.; Maragou, V.; Shen, P. K.; Tsiakaras, P. High Surface Area Tungsten Carbide Microspheres as Effective Pt Catalyst Support for Oxygen Reduction Reaction. *Appl. Catal., B* **2009**, *89*, 223–228.

(33) Wang, W.; Zheng, D.; Du, C.; Zou, Z.; Zhang, X.; Yang, B.; Akins, D. L. Carbon-Supported Pd-Co Bimetallic Nanoparticles as Electrocatalysts for the Oxygen Reduction Reaction. *J. Power Sources* **2007**, *167*, 243–249.

(34) Shao, M. H.; Sasaki, K.; Adzic, R. R. Pd-Fe Nanoparticles as Electrocatalysts for Oxygen Reduction. *J. Am. Chem. Soc.* **2006**, *128*, 3526–3527.

(35) Cheng, H.; Yuan, W.; Scott, K. The Influence of a New Fabrication Procedure on the Catalytic Activity of Ruthenium-Selenium Catalysts. *Electrochim. Acta* **2006**, *52*, 466–473.

(36) Mauritz, K. A.; Moore, R. B. State of Understanding of Nafion. *Chem. Rev.* **2004**, *104*, 4535–4586.

(37) Iwai, Y.; Yamanishi, T. Thermal Stability of Ion-Exchange Nafion N117CS Membranes. *Polym. Degrad. Stab.* **2009**, *94*, 679–687.

(38) Kerrec, O.; Devilliers, D.; Groult, H.; Marcus, P. Study of Dry and Electrogenated Ta<sub>2</sub>O<sub>5</sub> and Ta/Ta<sub>2</sub>O<sub>5</sub>/Pt Structures by XPS. *Mater. Sci. Eng.* **1998**, *B55*, 134–142.

(39) Wang, K.; Liu, Z.; Cruz, T. H.; Salmeron, M.; Liang, H. In Situ Spectroscopic Observation of Activation and Transformation of Tantalum Suboxides. *J. Phys. Chem. A* **2010**, *114*, 2489–2497.

(40) Lecuyer, S.; Quemerais, A.; Jezequel, G. Composition of Natural Oxide Films on Polycrystalline Tantalum Using XPS Electron Take-off Angle Experiments. *Surf. Interface Anal.* **1992**, *18*, 257–261.

(41) Thomas, J. H.; Hammer, L. H. A Photoelectron Spectroscopy Study of CF<sub>4</sub>/H<sub>2</sub> Reactive Ion Etching Residue on Tantalum Disilicide. *J. Electrochem. Soc.* **1987**, *136*, 2004–2010.

(42) Uekawa, N.; Mochizuki, N.; Kajiura, J.; Mori, F.; Wu, Y. J.; Kakegawa, K. Nonstoichiometric Properties of Zinc Oxide Nanoparticles Prepared by Decomposition of Zinc Peroxide. *Phys. Chem. Chem. Phys.* **2003**, *5*, 929–934.

(43) Li, Q.; Liang, C.; Tian, Z.; Zhang, J.; Zhang, H.; Cai, W. Core-Shell Ta<sub>x</sub>O@Ta<sub>2</sub>O<sub>5</sub> Structured Nanoparticles: Laser Ablation Synthesis in Liquid, Structure and Photocatalytic Property. *CrystEngComm* **2012**, *14*, 3236–3240.

(44) Eder, D.; Kramer, R. Stoichiometry of Titanium Suboxide. *Phys. Chem. Chem. Phys.* **2003**, *5*, 1314–1319.

(45) Macagno, V. A.; Schultze, J. W. The Growth and Properties of Thin Oxide Layers on Tantalum Electrodes. *J. Electroanal. Chem.* **1984**, *180*, 157–170.

(46) Puipe, J. C.; Leaman, F. *Theory and Practice of Pulse Plating*; American Electroplaters and Surface Finishers Society (AESF): Orlando, FL, 1986.

(47) Takasu, Y.; Kawaguchi, T.; Sugimoto, W.; Murakami, Y. Effects of the Surface Area of Carbon Support on the Characteristics of Highly-dispersed PtRu Particles as Catalysts for Methanol Oxidation. *Electrochim. Acta* **2003**, *48*, 3861–3868.

(48) Wang, G.; Sun, G.; Wang, Q.; Wang, S.; Cuo, J.; Gao, Y.; Xin, Q. Improving the DMFC Performance with Ketjen Black EC 300J as the Additive in the Cathode Catalyst Layer. *J. Power Sources* **2008**, *180*, 176–180.

(49) Denaro, T.; Baglio, V.; Girolamo, M.; Antonucci, V.; Arico, A. S.; Matteucci, F.; Ornelas, R. Investigation of Low Cost Carbonaceous Materials for Application as Counter Electrode in Dye-Sensitized Solar Cells. *J. Appl. Electrochem.* **2009**, *39*, 2173–2179.

(50) Xu, J. B.; Zhao, T. S. Mesoporous Carbon with Uniquely Combined Electrochemical and Mass Transport Characteristics for Polymer Electrolyte Membrane Fuel Cells. *RSC Adv.* **2013**, *3*, 16–24.

(51) Han, K.; Lee, J.; Kim, H. Preparation and Characterization of High Content Pt-Ru Alloy Catalysts on Various Carbon Blacks for DMFCs. *Electrochim. Acta* **2006**, *52*, 1697–1702.



(52) Inoue, H.; Hosoya, K.; Hannari, N.; Ozaki, J. Influence of Heat-Treatment of Ketjen Black on the Oxygen Reduction Reaction of Pt/C Catalysts. *J. Power Sources* **2012**, *220*, 173–179.

(53) Yin, F.; Takanabe, K.; Kubota, J.; Domen, K. Polymerized Complex Synthesis of Niobium- and Zirconium-Based Electrocatalysts for PEFC Cathodes. *J. Electrochem. Soc.* **2010**, *157*, B240–B244.